Numerical method for calculating input impedances of the oboe

George R. Plitnik

Department of Physics, Frostburg State College, Frostburg, Maryland 21532

William J. Strong

Department of Physics and Astronomy, Brigham Young University, Provo, Utah 84602
(Received 20 February 1978; revised 5 October 1978)

The purpose of this study was to investigate a numerical method for obtaining input impedances of double-reed instruments—the oboe in particular. To this end, the physical dimensions of an oboe were used to compute its input impedance as a function of frequency for several different fingerings. The numerically computed input impendances of the oboe were compared to experimentally measured curves with good agreement resulting in most cases. The reasons for the observed discrepancies are discussed and suggestions for improving the ageement between the predicted and experimental frequencies are given.

PACS numbers: 43.75.Ef

INTRODUCTION

A knowledge of the acoustic input impedance of woodwind instrument bores may be of considerable advantage in understanding their intonation, tonal quality, and the interaction of the reed with the bore. Furthermore, by determining the input impedance of actual instruments, intonation and tonal deficiencies could presumably be correlated with features of the input impedance. With an accurate method to calculate the input impedance of woodwind bores, a designer may, by calculating the effect of small changes in the bore taper and in the position or nature of tone holes, be able to predict how to improve the tone or intonation of an existing instrument.

Some general calculations have been made of the characteristic impedance of wind instrument bores. Using impedance methods, Morse[1] computed the resonance frequencies for a truncated cone representative of the double-reed bores. Because of assuming a constant end correction, his results predicted that the higher-mode frequencies are integral multiples of the fundamental frequency. However, experiments made by Bate and Wilson[2] have shown that the end correction for truncated cones is actually strongly frequency dependent, a fact which greatly complicates any computation of normal modes. Benade[3] extended the calculations of Morse to incorporate the frequency-dependent end corrections. He predicted that conical-bore instruments will have their normal modes spaced more widely than the harmonic series obtained by Morse. The original calculations show frequency shifts for the normal modes that are several orders of magnitude too small, but a recent erratum[4] provides results that are quantitatively correct. Experimental results of Backus[5] verify the direction and amount of frequency shift predicted.

Benade[6] also applied transmission line theory to bores having finger holes, but because of the tedious nature of the calculations for conical bores, he obtained only an approximate expression for the impedance of a clarinet (a cylindrical-bore instrument). Nederveen and de Bruijn[7,8] attempted to modify calculations for simple conical tubes to calculate the acoustical impedance of instruments with finger holes. Nederveen[8] also attempted to include the effect of viscous and thermal losses at the walls. However, the approximations that were made and the fact that the positions and details of the finger holes were not accounted for quantitatively, makes his results of doubtful value for any but the simplest oboelike structure. Young[9] used the digital computer for calculating the input impedance of smooth horns with no side holes or losses. However, it appears that Young's method does not easily lend itself to the inclusion of tone holes and losses due to the walls and is thus of limited value for woodwinds.

The current work represents an effort to apply numerical methods to the calculation of input impedances for woodwind bores with both losses and arbitrary placement of finger holes. Only conical-bore woodwind instruments are treated, but the method is basically applicable to cylindrical bores or to any combination of cylindrical- and conical-bore sections.

I. RATIONALE FOR THE IMPEDANCE CALCULATIONS

This section develops the procedure involved in calculating the bore impedance of woodwind instruments, from which normal mode frequencies can be determined. The theory of pressure disturbances in conical tubes is reviewed and used to derive the input impedance of simple lossless conical sections in terms of the impedance at the large end. Then, recent attempts that extend the theory of the bore impedance to take into account the reed impedance are reviewed. Finally, a numerical approach to the calculation of the input impedance of double-reed instruments with losses and finger holes is described.

A. Normal modes for lossless conical sections

In the double-reed instruments, air contained within a rigid conical tube is set into vibration by a pair of beating reeds whose frequency is determined by the interaction of the reeds with the normal modes of the air

 0001-4966/79/030816-10$00.80

column. To obtain a reasonably simple equation for the pressure disturbances within a tube of varying cross-sectional area S, the following assumptions are made[10]: (1) The fundamental acoustic equations for small displacements and small particle velocities are applicable; (2) the particle displacement and pressure are everywhere analytic functions of time and space; (3) the walls of the tube are rigid so that there is no transverse particle displacement at the walls; (4) the diameter is small compared to the wavelength of sound to be propagated, which implies that the phase remains approximately constant over every surface perpendicular to the axis of the tube; (5) the pressure varies sinusoidally with a frequency $\omega/2\pi$; and (6) the cross-sectional area S is proportional to x^2, where x is the distance along the axis.

With these assumptions, the funadmental lossless horn equation (in terms of the excess pressure) can be derived[11] as

$$\frac{d^2p}{dx^2}+\frac{2}{x}\frac{dp}{dx}+k^2p=0\ . \tag{1}$$

The solutions are

$$p(x)=\frac{A\exp(-jkx)+B\exp(jkx)}{x}\ , \tag{2}$$

where p now represents only the x-dependent part of the excess pressure, $k=\omega/c$, and A and B are complex constants.

The concept of acoustic impedance has proven useful in treating acoustical transmission systems. The input impedance of a conical section (i.e., the impedance at the throat or small end) can be derived in terms of the output impedance of the section (i.e., the impedance at the mouth or large end) and the length and flare of the section. The normal mode frequencies can then be computed by determining at what frequencies the input impedance achieves relative maxima for instruments in the double-reed class. The acoustic impedance at a point x can be written

$$Z(x)=p(x)/S(x)u(x)$$
$$=\frac{j\rho\omega}{x}\frac{[C\exp(-jkx)+\exp(jkx)]}{[C(1+jkx)\exp(-jkx)+(1-jkx)\exp(jkx)]}, \tag{3}$$

where C is a complex constant and where the particle velocity $u(x)$ has been defined as $(j/\rho\omega)(\partial p/\partial x)$.

The double-reed bores can be approximated as truncated conical sections where the diameter of the throat (small end) is much smaller than the diameter of the mouth (large end), as illustrated in Fig. 1. We can use Eq. (3) to define the impedance at the throat $Z_0=Z(x=x_0)$ and the mouth $Z_l=Z(x=x_0+l)$ of our truncated conical section. Then by eliminating the constant C between Z_0 and Z_l, the input impedance Z_0 is obtained after numerous manipulations as[12]

$$Z_0=\left(\frac{\rho c}{S_0}\right)\left\{jZ_l\left[\frac{\sin(kl-k\theta_2)}{\sin(k\theta_2)}\right]+\frac{\rho c}{S_l}\left[\sin(kl)\right]\right\}$$
$$\times\left\{Z_l\left(\frac{\sin(kl+k\theta_1-k\theta_2)}{\sin(k\theta_1)\sin(k\theta_2)}\right)-\frac{j\rho c}{S_l}\left[\frac{\sin(kl+k\theta_1)}{\sin(k\theta_1)}\right]\right\}^{-1}, \tag{4}$$

where $k\theta_1=\tan^{-1}(kx_0)$ and $k\theta_2=\tan^{-1}(kx_0+kl)$. To find the resonance frequencies of the cone, let $Z_l=R_l+jX_l$ (where R_l and X_l are the acoustic resistance and reactance at the mouth due to the radiation loading) and assume that $R_l\ll X_l$. A real denominator is obtained by multiplying the numerator and denominator by the complex conjugate of the denominator. Dropping terms in R_l^2, assuming that $k^2x_0(S_l+1)\gg 1$ and $ka\ll 1$, and representing[13] X_l as $0.6133(\rho\omega/\pi a)$, we set the denominator equal to zero to find where the impedance is a maximum. This leads to the transcendental equation

$$\tan(kl)=\frac{-kx_0(1+0.6133\,a/x_0)}{1-0.6133\,k^2ax_0}\ . \tag{5}$$

In Sec. IIB a numerical example is used to compare the frequencies predicted by Eq. (5) with those predicted by the more exact Eq. (4) and the resonance frequencies calculated numerically.

B. Effect of reed impedance

The pressure driving the reeds, supplied by the player, is common to the bore and the reeds. The incoming flow of air divides into two parts. One goes into the bore while the other fills the space left when the reed deflects. The reed impedance is then related to the airflow resulting from the reed deflection. From the above considerations, it is obvious that the reed acoustic impedance Z_r and the bore acoustic impedance Z_b should be added in parallel to give the input impedance to an actual instrument as $Z_i=Z_bZ_r/(Z_b+Z_r)$.

The simplest representation of the reed is to simulate the reed cavity and low-frequency reed compliance by a cavity of small volume. Since the cavity is located essentially at a velocity antinode and the frequencies of interest are fairly low, the reed can be approximately represented as a compliance. The acoustic impedance of the cavity can then be written as

$$Z=-j\rho c^2/\omega V\ . \tag{6}$$

The source impedance, equal primarily to the resistance of the small rectangular reed aperture, can be compared with typical values of the input impedance of the bore to determine whether the source acts more nearly as a constant-current generator or a constant-voltage source. Sivian[14] and Ingard and Ising[15] obtained expressions for the resistance of rectangular orifices in which the static volume flow of air is proportional to the pressure difference, which implies that the resistance is a constant. Measurements by Nederveen[8] verified that the preceding assumption is essentially correct for double reeds. Thus, the slit resistance can be written as $R_s=P/U$. Nederveen has provided a graph of the volume flow U as a function of stationary slit height for

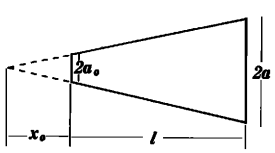

FIG. 1. Truncated conical section.

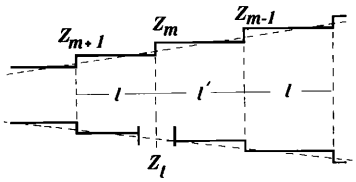

FIG. 2. Approximation of conical bore with contiguous cylindrical sections. Note finger hole between sections m and $m+1$.

oboe and bassoon reeds with various blowing pressures. From his data, the resistance is estimated to be in the neighborhood of 3000 Ω_{acoust} (cgs). The input impedance to the bore (in the region of maxima) is generally less than 1000 Ω_{acoust} (cgs). Thus, the volume flow (current) is essentially controlled by the slit impedance, making the reed a constant current generator. The maximum power output is obtained when the input impedance is maximum. The resonance frequencies occur when the magnitude of the input acoustic impedance is greatest, i.e., when the reactive component vanishes. At any resonance frequency, maximum power can be transmitted to the surrounding medium by the instrument. The effect of the reeds on the bore resonances can be gauged by adding the total reed impedance, given by the equations derived by Nederveen,[8] to the input impedance of the bore.

C. Numerical method for impedance calculation

None of the foregoing methods for determining the impedance of a truncated cone are easily applicable to the more general case where the cone does not involve the same flare parameter over its whole length, where losses must be included to achieve reasonable bandwidths, and where the placement and nature of the finger holes must be accounted for quantitatively. However, considerable success in calculating normal mode frequencies for vocal tracts with arbitrary shapes, losses, and side branches has been achieved by representing the tract with a series of short circular lossy cylinders.[16] This latter approach was adapted here to calculate the input impedances of double-reed instrument bores with a minimal number of approximations.

The conical bore is represented by a series of short circular cylinders as shown in Fig. 2. As the impedance at one end of a circular cylinder can readily be written in terms of the impedance at the opposite end and the dimensions of the cylinder, a straightforward method of obtaining the input impedance to the bore now presents itself. Let the impedance at the large end of the bore be the radiation impedance at a particular frequency f. This becomes the output impedance from which the input impedance (at the same frequency) is calculated for the first cylinder along the bore. The input impedance for the first cylinder then becomes the output impedance for the second cylinder, and the process is continued until the last cylinder is reached at the reed end of the bore. Whenever a tone hole is encountered, the appropriate impedance (which depends on whether the hole is opened or closed) is added in parallel to the net bore impedance at the center of the tone hole. When the input impedance of the final cylinder is computed, the input impedance of the entire bore is known at one frequency f. By repeating the above process at many different frequencies, a plot of impedance versus frequency may be constructed that represents the frequency dependence of the input impedance function. The cross-sectional areas of the bore and the position, size, and nature of the tone holes are determined by direct measurement and are input as data to a computer program.

At the large end of the tube, the radiation impedance was determined as a function of frequency, using the reaction on a rigid circular piston mounted in an unflanged cylindrical pipe of radius a obtained from expressions for the radiation resistance and reactance given by Beranek.[13] Beranek's expressions converted to the resistive and reactive components of the acoustic impedance of an unflanged cylindrical pipe of radius a are

$$R_r = 0.25\omega^2\rho/\pi c, \quad X_r = 0.6133\rho\omega/\pi a \,. \tag{7}$$

For an oboe, the requirement that $ka < 1$ insures accurate results for frequencies less than about 3000 Hz. Valid solutions are assured because $2a/\lambda$ does not exceed 1.2 for the frequencies of interest in double-reed instruments.

The conical bore of the oboe was approximated by a series of short circular cylinders. In order that the bandwidths as well as the resonance frequencies be accurately determined, the heat conduction and viscous losses were taken into account. This was accomplished by considering each cylinder as a section of lossy transmission line, where the input impedance Z_0 is given by

$$Z_0 = Z_c[Z_l + Z_c \tanh(\gamma l)]/[Z_c + Z_l \tanh(\gamma l)] \,, \tag{8}$$

at each frequency, and where Z_c is the characteristic impedance, γ is the propagation constant, and l is the length of the section. These parameters are given as

$$Z_c = [(R + j\omega L)/(G + j\omega C)]^{1/2},$$
$$\text{and } \gamma = [(R + j\omega L)(G + j\omega C)]^{1/2} \,, \tag{9}$$

with L representing inertance, C representing compliance, R representing viscous losses, and G representing heat conduction losses; they are given by[16]

$$L = \rho/S, \quad C = S/\rho c^2 \,,$$
$$R = 2\pi(\rho\mu f/S^3)^{1/2} \text{ and } G = [2\pi(\eta - 1)/\rho c^2](\lambda f S/\rho h)^{1/2} \,, \tag{10}$$

where μ is viscosity of air, η is the ratio of specific heats, λ is the coefficient of heat conduction, ρ is air density, c is sound speed in air, h is specific heat at constant pressure, and S is cross-sectional area. For the option of a lossless case, the above equations would be considerably simplified.

The impedance of the finger holes are added in parallel at the appropriate points as in Fig. 2. For an open finger hole the resistive part of the radiation impedance is approximated by the impedance function for a rigid circular piston mounted in an infinite baffle. If a is the

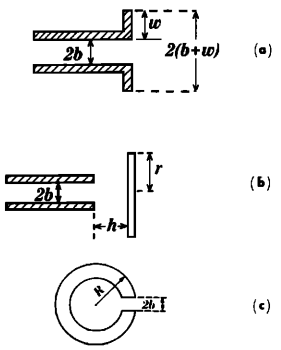

FIG. 3. Tone hole terminations: (a) flanged end; (b) disk in front of open end; (c) outer surface of instrument serves as flange. (After Benade and Murday, see Ref. 18.)

radius of the piston and $y = 4\pi a/\lambda$, then when $y < 0.85$ the resistive impedance function[17] $R_1(y)$ can be represented to an accuracy of at least 0.1% by the truncated series

$$R_1(y) = \tfrac{1}{8}y^2 - \tfrac{1}{192}y^4 + \tfrac{1}{9216}y^6, \text{ and } R_r = (\rho c/\pi a^2)R_1(y) . \quad (11)$$

The reactive part of the tone hole impedance is given by

$$X_r = (2\rho f/a^2)\Delta l , \quad (12)$$

where Δl is a length correction for an open tone hole which is given by one of the expressions in Eq. (13)[18] depending on the manner in which the hole is terminated as illustrated in Fig. 3:

$$\Delta l = b[0.821 - 0.13(w/b + 0.42)^{-0.54}] , \quad (13a)$$

$$\Delta l = b[0.61(r/b)^{0.18}(b/h)^{0.39}] , \quad (13b)$$

$$\Delta l = b \times 0.64[1 + 0.32\ln(0.30R/b)] . \quad (13c)$$

There is some question[18] about the need for an additional end correction to account for the inside end of the hole when Eq. (13c) is used. Only the expression shown in Eq. (13c) was used in this study, which may be a source of error. Also, Eqs. (11)–(13) do not take into account interactions with neighboring open holes and this may be a source of error. However, the good agreement between theory and experiment shown later in Sec. II D indicates that the effects are small. For a closed finger hole, it is assumed that Z_t is infinitely large. It can then be shown from Eq. (8) that $Z = Z_c/\tanh(\lambda l)$ is the input impedance for a lossy closed finger hole of length l.

The input impedance of the $(m+1)$st section with a finger hole at its output (as in Fig. 2) is given by

$$Z_{m+1} = Z_c[Z'_m + Z_c\tanh(\gamma l)]/[Z_c + Z'_m\tanh(\gamma l)] , \quad (14)$$

where

$$Z'_m = Z_m Z_t/(Z_m + Z_t) , \quad (15)$$

in which Z_m is the input impedance of section m and Z_t is the input impedance of the finger hole.

II. RESULTS OF THE IMPEDANCE CALCULATIONS

This section presents the results of utilizing the impedance method, described in Sec. I C, to compute numerically the input impedance of oboe bores. A description of the computer program on which all the computations were performed is given first. Then, the validity of the method described in Sec. I C is shown for simple truncated cones and compared with results predicted by the "exact" equations. Next, the effects of gradually modifying the complexity of the cone (until it became a reasonable facsimile of an actual oboe bore) were determined. Finally, the computed impedance characteristics for various fingerings on an actual oboe are compared with the corresponding experimental data.

A. Description of the computer program

The computer program IMPED was written in FORTRAN and used to compute and plot the magnitude of the input impedance of woodwind bores as a function of frequency. (As woodwind instruments are composed of several individual pieces which join together, the word "joint" was used in this program to represent each of these individual pieces.) The control variables for the computer program were as follows: loss/no-loss option, number of joints in the tube, number of side holes in the tube, the frequency increments in the calculations, the diameter of the mouth of the tube, the maximum length of each cylindrical section, the volume of the mouthpiece cavity, the air temperature, the difference of end diameters for each joint in the tube, and the length of each joint. The diameter and length of the side holes and the distance of the center of the side hole from the bell were also included when present, along with a specification of which tone holes were open. The distance of the small end of each joint from the end of the bell was also given.

Starting with the first frequency given in the input data, the program computed the input impedance at frequencies spaced five Hz apart. The air constants for use in the cylindrical section calculations were computed for the temperature assumed. For each frequency the program began at the bell with the radiation impedance and proceeded to calculate the input impedance for each cylindrical section using Eq. (8). When tone holes were included, the calculations were identical, except that when a hole was encountered the section length l' for this cylinder was chosen such that the section terminated at the center of the side branch, under the restriction that $l' \leq l$. When the tone hole was open, its radiation impedance was included and the input impedance of the side branch was calculated. If the tone hole was closed, the radiation impedance was taken to be infinite. In either case, the total impedance at the side branch was then computed by adding in parallel the bore impedance at that point and the impedance of the tone hole.

When the input impedance to the entire bore had been calculated at a particular frequency, it was added in parallel to the reed cavity impedance, which was computed from Eq. (6). The log magnitude of the impedance is here called the relative impedance level in decibels; it is "relative" because the reference impedance is arbitrary. It is computed at each desired frequency by $10\log(R^2 + X^2)$, where R and X are respectively the real and imaginary parts of the complex impedance. The

TABLE I. The effect on frequency (in hertz) of varying the section length in the impedance program.

$L = 1.0$ cm	$L = 0.5$ cm	$L = 0.25$ cm
256.0	256.0	256.0
512.0	513.0	513.0
770.0	772.0	772.0
1030.0	1033.0	1033.0
1290.5	1296.0	1296.5
1553.0	1561.0	1561.5
1817.5	1827.5	1827.5
2082.0	2095.0	2095.5
2347.5	2364.0	2364.0
2614.5	2633.0	2633.5
2881.5	2903.0	2903.5

impedance level and the frequency at which it was computed were then stored until sufficient data had been accumulated to plot impedance level versus frequency.

B. Validity of the numerical computation of impedance

The method of computing the input impedance of a woodwind bore, developed in Sec. IC assumed that the bore may be approximated by a series of short cylindrical sections. To check the validity of this assumption, a simple truncated cone with no losses and no finger holes was modeled on the computer. As a first approximation to an oboe, the length l was chosen equal to the length of a Strasser oboe with a reed staple in place but without the reed. Also, the diameter of the small end of the cone $2a_0$ and the diameter of the large end $2a$ were made equal to the respective end diameters of the oboe. The dimensions of the cone were then $l = 62.53$ cm, $2a = 3.64$ cm, $2a_0 = 0.23$ cm, and $x_0 = 4.22$ cm.

To determine the optimum length of the cylindrical sections to be used in the representation of the cone, three runs were made with the maximum section lengths l being 1.0, 0.5, and 0.25 cm. The results (from 0 to 3000 Hz) are tabulated in Table I, where f is the frequency in hertz at which the peaks occurred in the impedance function. The frequency data are accurate to ± 0.5 Hz because increments of 1 Hz were used in the program. Consideration of Table I shows that $l = 0.5$ cm is the optimum section length for the oboe, since use of shorter section gives almost the same results but requires more computation time.

TABLE II. Normal-mode frequencies, in hertz, of the simple truncated cone.

Harmonic	IMPED	Eq. (4)	Eq. (5)
256.0	256.0	256.0	256.0
512.0	513.0	513.0	513.2
768.0	772.0	772.0	772.2
1024.0	1033.0	1033.0	1033.4
1280.0	1296.0	1296.0	1296.6
1536.0	1561.0	1561.0	1561.7
1792.0	1827.5	1827.5	1828.4
2048.0	2095.0	2095.0	2096.3
2304.0	2364.0	2363.0	2365.3
2560.0	2633.0	2632.5	2635.3
2816.0	2903.0	2903.5	2905.8

TABLE III. Dimensions of oboe joints.

Joint	Length (cm)	Diameter large end (cm)	Diameter small end (cm)	Distance from bell to small end (cm)
Bell	7.32	3.64	1.90	7.32
Bell	7.53	1.90	1.50	10.85
Lower	23.83	1.50	1.02	34.68
Upper	23.17	1.02	0.40	57.85
Staple	4.68	0.47	0.23	62.53

Having determined the optimum section length for the calculations, the simple truncated cone dimensions given in the preceding paragraph were then used to compare the resonance frequencies predicted by IMPED with those predicted by Eqs. (4) and (5). The frequencies (to ± 0.5 Hz) at which the impedance maxima occurred for IMPED and Eq. (4) are listed in the second and third columns of Table II. In column 4 the roots of transcendental Eq. (5), which predicts the resonance frequencies of a truncated cone (to ± 0.2 Hz) under the limitations discussed in Sec. IA, are tabulated. The first column, labeled "Harmonic," lists the integral multiples of the fundamental frequency for comparison.

Inspection of the table yields the following pertinent information: (1) the agreement between IMPED and Eq. (4) is excellent; (2) the agreement between these "exact" solutions and Eq. (5) is very good, Eq. (5) giving frequencies about 0.1% too high for the upper harmonics; (3) the resonance frequencies are stretched from integral multiples of the fundamental as predicted earlier.

From this information it can be seen that the approximations made in Sec. IA to obtain Eq. (5) are not unreasonable and the computer program IMPED can be used validly to predict the normal modes of truncated cones. Based on the second conclusion, the underlying assumption of this work is that woodwind bores of any degree of complexity (with losses and tone holes) can be represented accurately by the computer program IMPED.

C. Impedance calculation for a modified simple cone

Modifications to the simple truncated cone were based on measurements of a Strasser oboe. The dimensions of the three oboe joints and the reed staple are given in Table III. The measurements were made with a vernier caliper, a micrometer, and a meter stick. Dimensions and other details of the finger holes are given in Table IV.

The first modification to the simple truncated cone was to represent the bore (with staple) as five conical joints. As can be seen in Table III, the oboe bore consisted of a conical reed staple, two conical joints, and a bell. Since the bell flares somewhat at the end, it was represented as two conical joints. This then gave a total of five joints. The end diameters and the length of each joint were input parameters to the computer program. The diameter at any distance from the bell was then computed by linear interpolation, under the

TABLE IV. Description and dimensions of oboe finger holes.

Hole no.	Type	Location (joint)	Bell-to-hole center distance (cm)	Hole diameter (cm)	Hole length (cm)	Cap diameter (cm)	Flange length (cm)	Ht. open cap	Hole in cap, diameter (cm)
1	cap	bell	9.72	1.1	0.6	1.30		0.3	
2	cap	lower	13.72	1.0	0.6	1.30		0.3	
3	cap	lower	17.11	0.70	0.6	1.00		0.3	
4	cap	lower	20.57	0.90	0.6	1.20		0.3	
5	cap	lower	23.60	0.72	0.6	1.00		0.3	
6	hole	lower	27.59	0.60	0.85		0.36		
7	cap	lower	29.24	0.66	0.6	0.95		0.3	
8	cap–hole	lower	30.49	0.82	0.6	1.20		0.3	0.10
9	cap	lower	32.06	0.52	0.60	0.80		0.3	
10	hole	lower	34.03	0.60	0.85		0.35		
11	cap	upper	36.97	0.45	0.65	0.75		0.3	
12	hole	upper	40.04	0.42	0.95		0.44		
13	cap	upper	41.60	0.50	0.6	0.75		0.3	
14	hole	upper	43.35	0.39	0.95		0.42		
15	cap	upper	44.42	0.32	0.6	0.75		0.3	
16	cap–hole	upper	46.23	0.22	0.6	0.95		0.3	0.10
17	cap	upper	47.42	0.36	0.6	0.75		0.3	
18	cap	upper	48.45	0.36	0.65	0.75		0.3	
19	cap	upper	51.41	0.26	0.70	0.70		0.3	
20	cap	upper	57.02	0.26	0.70	0.70		0.3	

assumption that each joint was a simple truncated cone. This assumption was generally valid for all joints except the terminating section of the bell joint, which is flared somewhat. (A closer approximation to this flared section was obtained by representing the oboe bell by four conical joints rather than two. This was done and comparison of frequency data for complete bores of five and seven conical joints showed them to be identical within 0.2%.) For each case it was assumed that there were no discontinuities in diameter where two joints meet. In actuality, there was a prominent discontinuity at the junction of the staple and the bore. This effect is examined later. Meanwhile, the end diameter of the staple (0.47 cm) was used as the diameter of the small end of the upper joint, so that the bore was continuous. An examination of Table V shows that there is considerable difference in the results between the cones of one and five joints.

Representing the bore with five joints, the following changes to the smooth bore were introduced sequentially: (1) The discontinuity between the bore and the staple was included, (2) closed tone holes were included, (3) the reed cavity was added, and (4) the losses were taken into account. The effects of each of these changes can be gauged by considering Table V, where each modification includes all of the previous ones. The discontinuity between the bore and the staple, as discussed earlier, had the effect of raising the normal mode frequencies. This was because the cross-sectional area in the upper part of the top joint had been decreased. Adding the closed tone holes (see Table IV for data), which had the effect of increasing the effective cross-sectional area of the bore, lowered the normal mode frequencies. The reed cavity volume and low-frequency reed compliance had the effect of lowering the resonance frequencies of the high-frequency modes. Finally, the incorporation of losses did not significantly affect the normal mode frequencies, even though there was a profound effect upon the amplitudes and bandwidths of the peaks.

D. Comparison with experimental data

Experimental curves were made on the same Strasser oboe by A. H. Benade in July 1970 using an impedance measuring apparatus equipped with a Coltman-type impedance head as described in the literature.[19] Figures 4–12 present a comparison of relative input impedance levels for nine different notes in the low register of the oboe. The upper curve in each figure is experimental; the lower curve is calculated. The experimental and calculated impedance levels are based on different arbitrary reference impedances, so their absolute values may not be compared directly. However, rather

TABLE V. Normal-mode frequencies, in hertz, for modifications to the simple cone.

One joint	Five joints (continuous)	Discontinuity at staple	Closed holes	Reed cavity	Losses
256.0	241.0	246.5	234.0	230.0	230.0
513.0	517.0	523.0	504.0	481.0	480.5
772.0	793.0	788.0	762.0	708.0	707.5
1033.0	1058.5	1049.0	1003.0	938.0	938.0
1296.0	1302.0	1289.0	1244.0	1174.5	1175.5
1561.0	1557.0	1543.0	1496.0	1388.5	1391.5
1827.5	1827.5	1814.5	1750.5	1620.5	1626.5
2095.0	2102.0	2093.0	2018.0	1860.0	1868.0
2364.0	2372.5	2369.5	2281.0	2123.5	2134.5
2633.0	2638.0	2640.5	2535.0	2384.0	2397.0
2903.0	2906.0	2915.0	2800.0	2631.0	2645.0

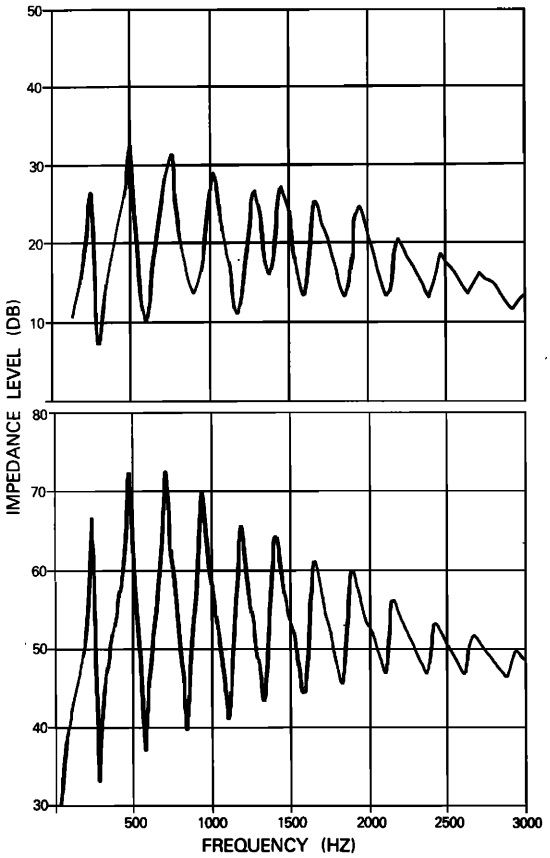

FIG. 4. Experimental (upper) and calculated (lower) relative input impedance levels for oboe note B3.

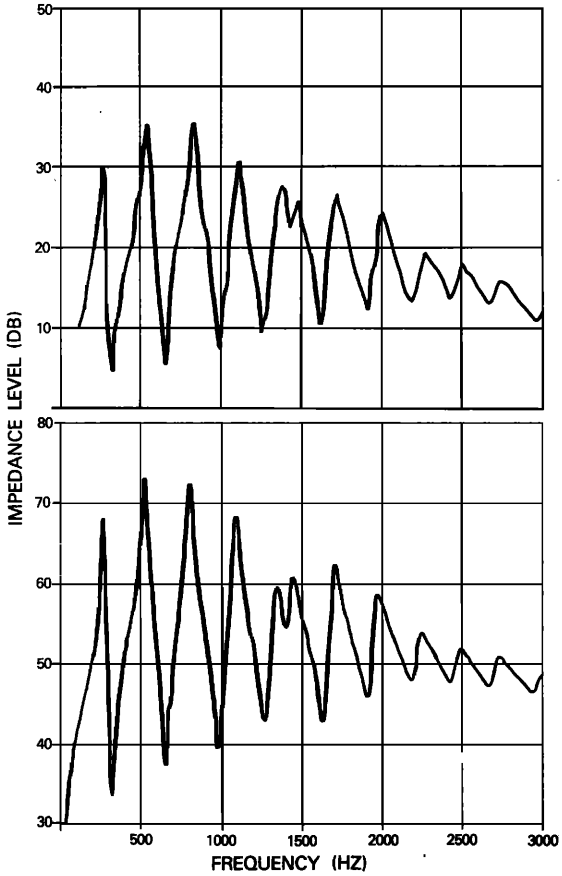

FIG. 5. Experimental (upper) and calculated (lower) relative input impedance levels for oboe note C4.

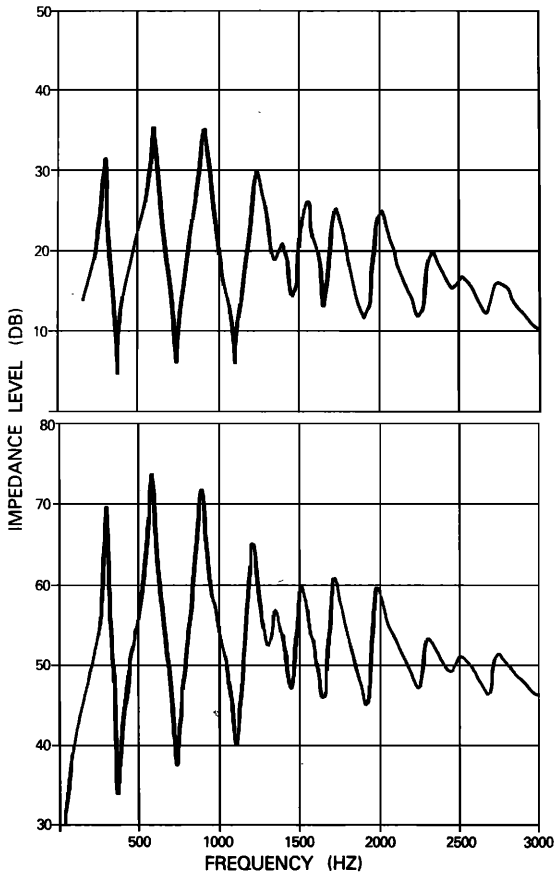

FIG. 6. Experimental (upper) and calculated (lower) relative input impedance for oboe note D4.

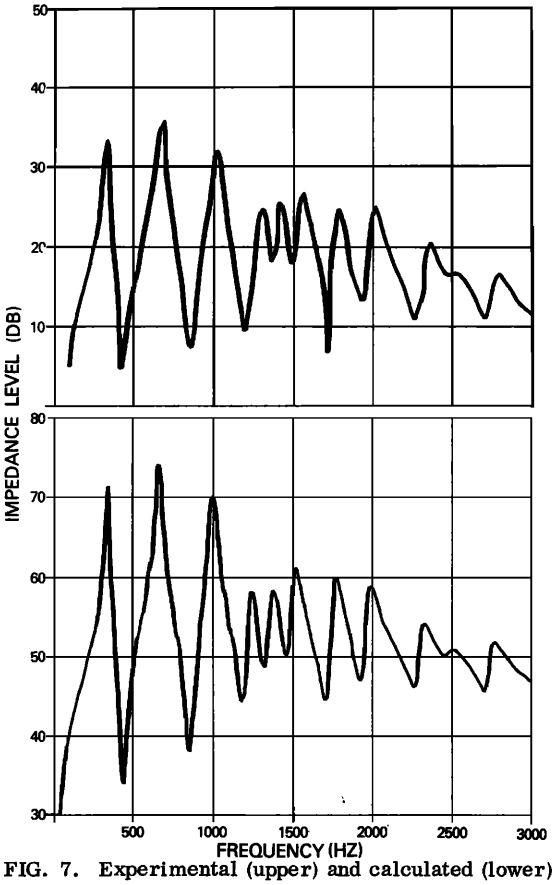

FIG. 7. Experimental (upper) and calculated (lower) relative input impedance levels for oboe note E4. (From Strong and Plitnik.[20])

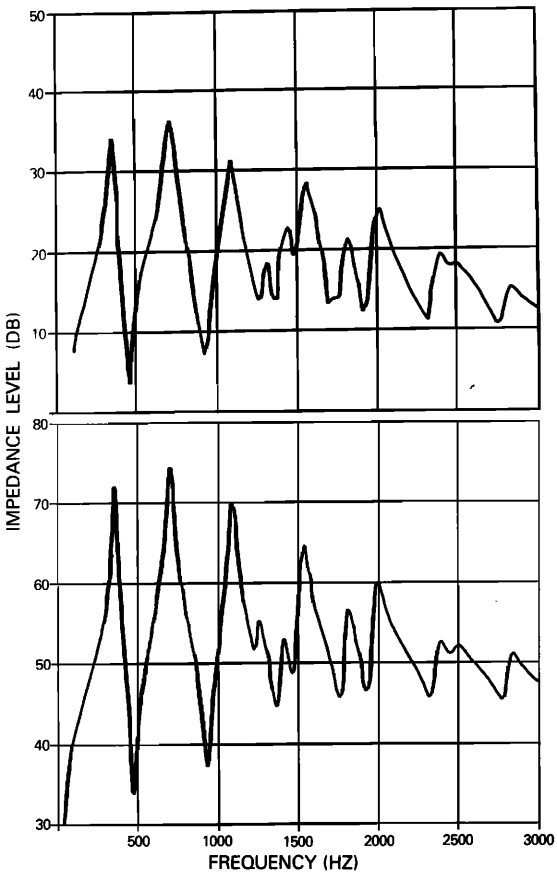

FIG. 8. Experimental (upper) and calculated (lower) relative input impedance for oboe note F4.

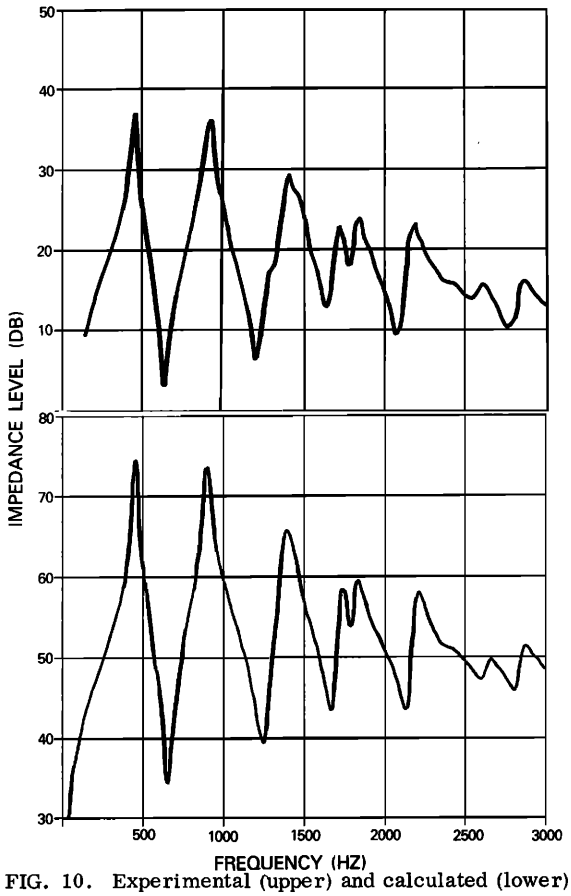

FIG. 10. Experimental (upper) and calculated (lower) relative input impedance levels for oboe note A4.

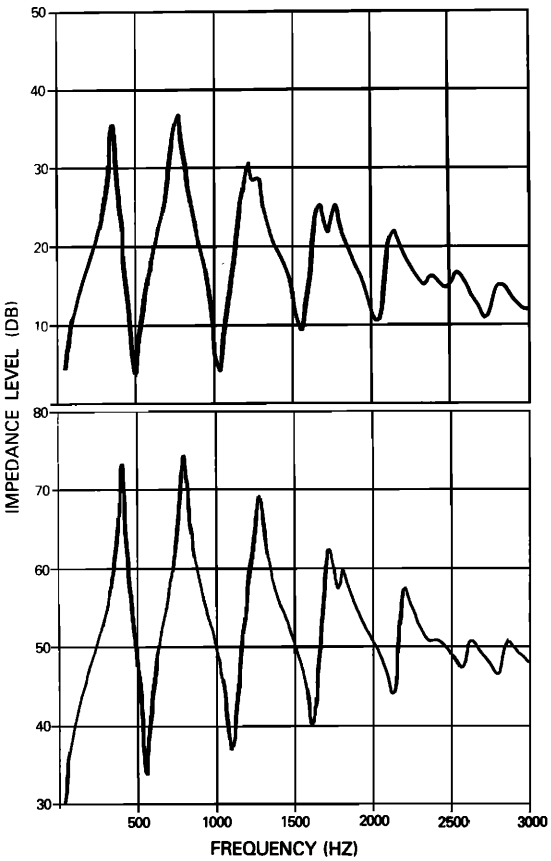

FIG. 9. Experimental (upper) and calculated (lower) relative input impedance levels for oboe note G4. (From Strong and Plitnik.[20])

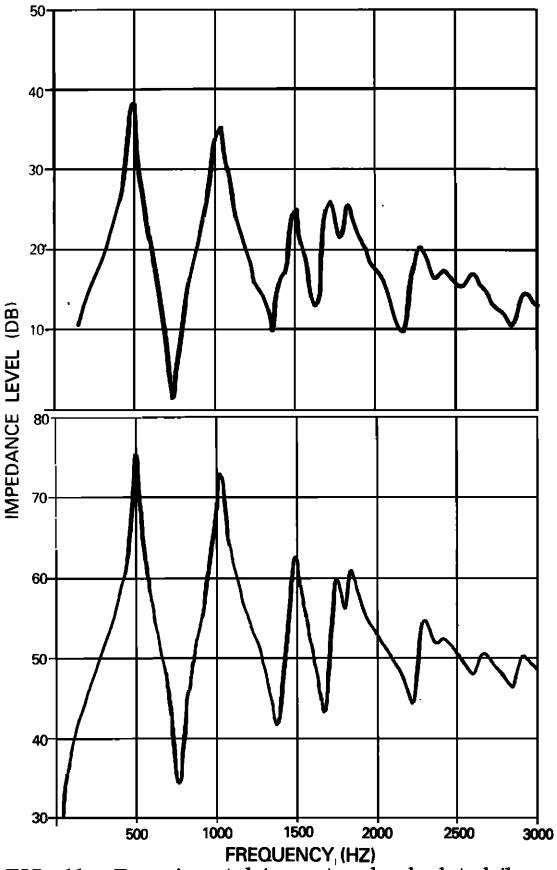

FIG. 11. Experimental (upper) and calculated (lower) relative input impedance levels for oboe note B4. (From Strong and Plitnik[20].)

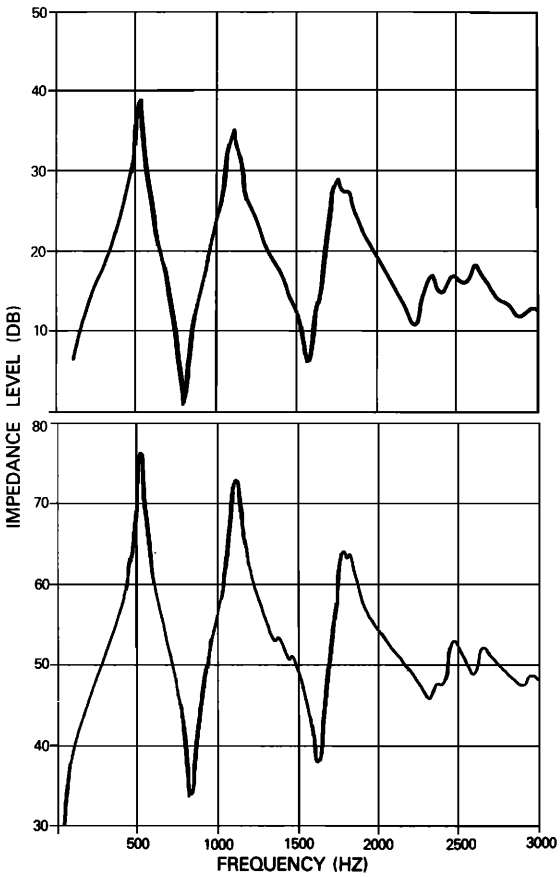

FIG. 12. Experimental (upper) and calculated (lower) relative input impedance levels for oboe note C5.

meaningful comparisons can be made in terms of relative positions, heights, and details of corresponding peaks. Note the close similarity in the curves; the major difference is that the peak-to-dip changes in impedance levels are systematically larger for the calculated than for the measured impedance levels; this indicates that there are energy losses present in the real oboe which we did not incorporate into the computer program. Three such mechanisms may possibly explain this discrepancy. First, we assumed (incorrectly) that the pads or fingers covering a closed tone hold form an infinite impedance termination. In fact, the pads are somewhat porous and both pads and fingers are somewhat flexible, thus consuming some acoustic energy. Second, the socket and tenon junctions also consume energy since they provide large areas of air surface that have a (0.1 mm thick) boundary layer surface constrained on both sides of fairly closely fitting pieces of wood and cork. These joints can account for several percent of the total wall loss. Finally, an additional energy sink in a woodwind comes from the presence of many corners and edges where tone holes intersect the bore, as well as in the socket and tenon junctions of the various pieces. It is known[21] that the dissipation per unit area of these strongly curved surfaces is considerably more than that of a flat surface.

The input impedance curve of an oboe has several characteristic features which help determine the tone and playing behavior of the instrument. There are usually two or more "normal-appearing" resonance peaks at low frequencies. At higher frequencies, beyond the open-hole cutoff frequency, the added length of air column leads to a considerable irregularity in the spacing, shape and height of peaks. The cutoff frequency can be observed by inspection of Figs. 5–11, which show cutoff frequencies in the range of about 1300–1700 Hz. In Fig. 12 the cutoff frequency apparently lies above 2000 Hz. For the lower notes of the oboe's range, such as in Figs. 5 and 6, there are fewer holes open and the transition is less readily observed. Figure 4 indicates that for this low note the impedance curve looks remarkably similar to that of a brass instrument.

For an oboist to achieve a good, clear tone in the low register, it is crucial that the frequencies of two or three impedance peaks lie very near to integral multiples of the played pitch frequency. When a reed is placed on the oboe, the frequencies of peaks beyond the first are lowered slightly. Therefore, on a well-designed instrument the impedance peaks measured in the above manner should be just the right amount sharp to offset the effect of the reed. By inspecting the impedance curves, we discover that among the top five notes, all are fairly good (having three well-tuned peaks), except that shown in Fig. 11. This figure shows shows an impedance curve for a relatively bad note (B4) in which the third peak is missing. Figure 7 shows the impedance curve for a particularly bad note (E4) on this oboe; even though the third peak is present, it is, in fact, somewhat flat. Figure 6 gives the plot of a very good note (D4) in which a well-tuned fourth peak makes it louder and brighter than its neighbors.

Figure 13 shows the calculated result of opening one additional hole (No. 9) which is below the highest open hole for the note C5 as in Fig. 12. Observe that opening the extra hole splits the important third peak into several peaks of reduced amplitude. A comparison of Figs. 12 and 13 indicates that the third peak is a nearly degenerate superposition of peaks which is resolved when hole No. 9 is opened. Even though hole No. 9 is open for several notes below C5, it is important for the

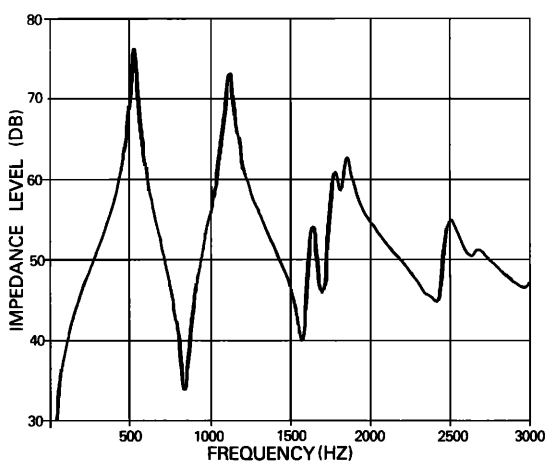

FIG. 13. Calculated relative input impedance level for oboe note C5, with modified fingering.

production of a good clear tone that it be closed when C5 is played.

E. Summary and projections

We have shown that the computer program IMPED accurately predicts salient features of the impedance curves of an actual oboe. It may be that the program can be utilized to predict the resulting change to the input impedance when modifications are made to the bore of an oboe with poorly placed resonance peaks. By use of this method, nondestructive experiments could be conducted on an oboe to determine if the peak placement (and consequently the sound) of certain notes could be improved by modifications to selected parts of the bore.

A logical extension of this work would be to attempt to achieve optimum placement and size of the finger holes and optimum variation of internal bore diameter. The optimization of these parameters could be accomplished by using a multivariable search technique program, such as those often used in industrial research. Such parameter optimization, when applied to double-reed instruments, might enable one to construct instruments with more uniform and improved tone quality over the entire playing range.

ACKNOWLEDGMENTS

We are indebted to A. H. Benade for providing us with experimental impedance curves for the Strasser oboe studied. He also played selected notes on the oboe and provided us with comments on their musical behaviors and impedance curves which we have included. Also, we express our thanks to A. H. Benade and J. Backus for helpful discussions on impedance measuring techniques and the interpretation of impedance curves. A special word of appreciation is due to Ed Pfrang for assistance in implementing the computer program and for many helpful discussions. We thank the two reviewers of the manuscript who provided many insightful and helpful comments.

[1]P. M. Morse, *Vibration and Sound* (McGraw–Hill, New York, 1948), 2nd ed., p. 287.
[2]A. E. Bate and E. T. Wilson, "Resonance in Truncated Cones," Philos. Mag. **26**, 752–757 (1938).
[3]A. H. Benade, "On Woodwind Instrument Bores," J. Acoust. Soc. Am. **31**, 137–146 (1959).
[4]A. H. Benade, "On Woodwind Instrument Bores," reprinted in *Musical Acoustics: Piano and Wind Instruments* (Dowden, Hutchinson, and Ross, Stroudsburg, PA, 1977).
[5]J. Backus, "Input Impedance Curves for the Reed Woodwind Instruments," J. Acoust. Soc. Am. **56**, 1266–1279 (1974).
[6]A. H. Benade, "On the Mathematical Theory of Woodwind Finger Holes," J. Acoust. Soc. Am. **32**, 1591–1608 (1960).
[7]C. J. Nederveen and A. de Bruijn, "Hole Calculations for an Oboe," Acustica **18**, 47–57 (1967).
[8]C. J. Nederveen, *Acoustical Aspects of Woodwind Instruments* (Knuf, Amsterdam, 1969).
[9]F. J. Young, "The Natural Frequencies of Musical Horns," Acustica **10**, 91–97 (1960).
[10]G. W. Stewart and R. B. Lindsay, *Acoustics* (Van Nostrand, New York, 1930), p. 134.
[11]A. G. Webster, "Acoustical Impedance, and the Theory of Horns and of the Phonograph," Proc. Natl. Acad. Sci. US **5**, 275–282 (1919).
[12]H. F. Olson, Acoustical Engineering (Van Nostrand, New York, 1957), pp. 106–107.
[13]L. Beranek, *Acoustics* (McGraw–Hill, New York, 1954), p. 125.
[14]L. J. Sivian, "Acoustic Impedance of Small Orifices," J. Acoust. Soc. Am. **7**, 94–101 (1935).
[15]U. Ingard and H. Ising, "Acoustic Nonlinearity of an Orifice," J. Acoust. Soc. Am. **42**, 6–17 (1967).
[16]J. L. Flanagan, *Speech Analysis, Synthesis, and Perception* (Academic, New York, 1972), 2nd ed.
[17]L. E. Kinsler and A. R. Frey, *Fundamentals of Acoustics* (Wiley, New York, 1962), 2nd ed., p. 179.
[18]A. H. Benade and J. S. Murday, "Measured End Corrections for Woodwind Tone Holes," J. Acoust. Soc. Am. **41**, 1609 (1967).
[19]A. H. Benade, "The Physics of Brasses," Sci. Am., 24–35 (July 1973).
[20]W. J. Strong and G. R. Plitnik, *Music, Speech, and High-Fidelity* (Brigham Young U. P., Provo, UT, 1977).
[21]A. F. Kuckes and U. Ingard, "Note on Acoustic Boundary Dissipation Due to Viscosity," J. Acoust. Soc. Am. **25**, 798(L) (1953).